ACS Catalysis

Research Article

pubs.acs.org/acscatalysis

Understanding the Chemistry of H_2 Production for 1-Propanol Reforming: Pathway and Support Modification Effects

Rodrigo Lobo,[†] Christopher L. Marshall,*[,†] Paul J. Dietrich,[§] Fabio H. Ribeiro,[§] Cem Akatay,[§] Eric A. Stach,[∥] Anil Mane,[‡] Yu Lei,[‡] Jeffrey Elam,[‡] and Jeffrey T. Miller[†]

[†]Chemical Sciences and Engineering Division and [‡]Energy Systems Division, Argonne National Laboratory, Argonne, Illinois 60439, United States

[§]School of Chemical Engineering, Purdue University, West Lafayette, Indiana 47907, United States

[∥]Center for Functional Nanomaterials, Brookhaven National Laboratory, Upton, New York 11973, United States

ABSTRACT: The liquid-phase reforming of 1-propanol over a platinum-based catalyst on a number of supports was investigated. Propanol is being used as a surrogate for biomass-derived glycerol as a source of hydrogen in the conversion of cellulose to transportation fuels. The test conditions were high temperature (230−260 °C) and pressure (69 bar) in the presence of liquid water. Under these conditions, Pt over alumina coated (via atomic layer deposition) with a layer of approximately 1 nm of Al_2O_3, TiO_2, or Ce_2O_3 (Pt−Al, Pt−Ti, Pt−Ce) is active for the reforming of 1-propanol. The Pt−Ti catalyst had the highest 1-propanol conversion rate per gram of catalyst followed by the Pt−Al and Pt−Ce catalysts, which had similar rates of reaction. Selectivity for each catalyst was primarily to ethane and CO_2, with the ratio between the two products being close to unity regardless of temperature. The hydrogen yield was constantly higher than twice the ethane yield, indicating that H_2 formation occurs before ethane is formed. Decarbonylation of propanal did not appear to contribute significantly to the formation of ethane. The propionic acid, which can produce ethane and CO_2 through decarboxylation, is believed to form from the disproportionation of propanal. In contrast to the Canizzarro reaction, this reaction appears to be catalyzed by the supported Pt and not the support or in solution (through base catalysis). Our analyses also showed that well dispersed Pt sinters under the high temperature and high partial pressure of water in the reactor, and under reaction conditions that the surface of the Pt has high concentrations of CO (43% of the coverage of CO at room temperature) and water (96% of the coverage of water at 230 °C and 34 bar).

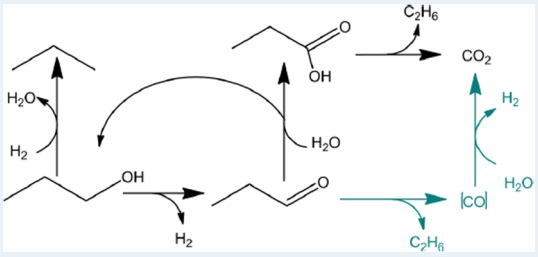

KEYWORDS: *biomass, Pt catalysts, liquid phase reforming, EXAFS, XANES*

1. INTRODUCTION

Replacement of fossil sources for the generation of fuels from biologically derived feedstocks has several challenges that still need addressing. These fuel challenges include incompatibility with current engines, high variability within the feedstock source, product, and method of pretreatment. The raw biomass can be insoluble with current fuels because of the presence of large amounts of "organic oxygen."[1−3] Thus, it is desirable to remove most if not all of the oxygen from these organic compounds to produce a more stable product with both a higher energy content (less oxidized) and a chemical structure closer to that of current fossil fuels.

A major challenge to achieving deoxygenation of biological feedstocks is not the ability to perform the reactions, but the need for large quantities of hydrogen to do so.[4−8] Although hydrogen is readily available at refineries and petrochemical plants, this hydrogen originates from fossil sources, and if used for upgrading, the biofuels would be both dependent on petroleum availability and would not be carbon neutral. Furthermore, since the processing of biological feedstocks will primarily be local (<200 km radius), in most cases this processing would be done far from the hydrogen produced by petrochemical plants.

Among the most viable solutions is the generation of hydrogen from the biofeedstocks, particularly if it can be produced from byproducts of other processes. Glycerol, a byproduct in the production of biodiesel, would be an example of such a feedstock. Typically, to obtain H_2 (as opposed to H_2O) from the conversion of such a molecule requires the use of a supported metal catalyst. In addition to being mechanically stable and easily separated from products, supported metal catalysts allow tuning of the product distribution by changing both the support material and the type of catalytic metal.

The production of hydrogen from molecules like glycerol and glycol (i.e., reforming) has been studied.[9] However, in most cases these studies have focused only on the production of hydrogen with little mechanistic data. In other studies many

Special Issue: Operando and In Situ Studies of Catalysis

Received: June 22, 2012
Revised: August 13, 2012
Published: September 17, 2012

   dx.doi.org/10.1021/cs300405s | *ACS Catal.* 2012, 2, 2316−2326

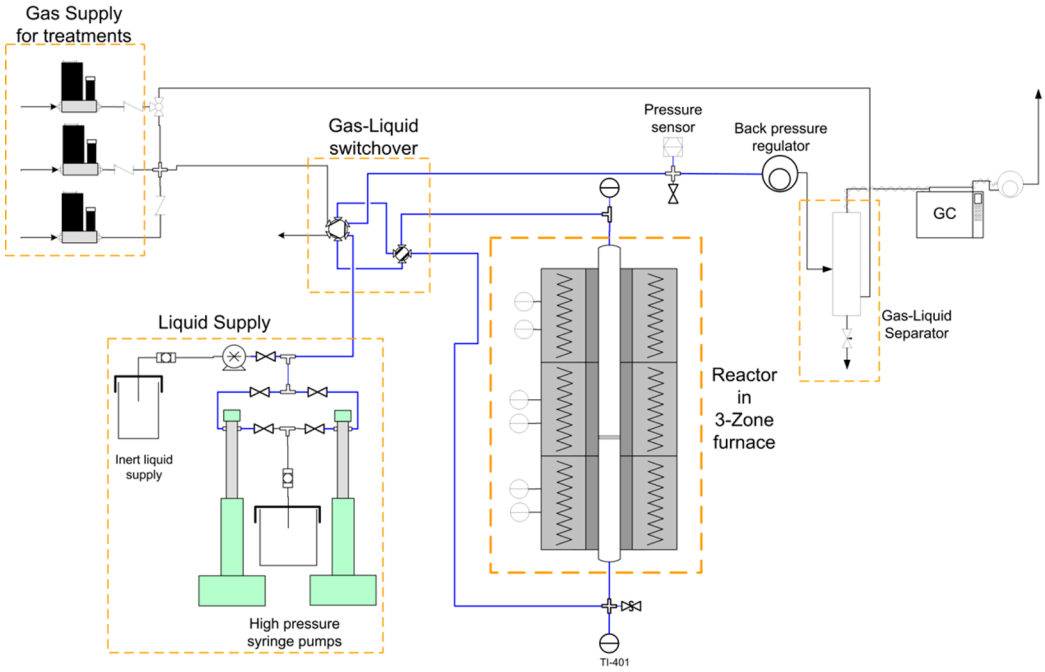

Figure 1. High pressure reactor system used for pretreatment and catalyst testing studies.

of the intermediate compounds formed during reforming of such molecules were identified and quantified.[10−13] A limitation of this approach is that the number of compounds produced during reforming prevents a detailed understanding of the reaction pathway leading to hydrogen formation. In this paper we focus on a simple molecule, 1-propanol, with the aim of understanding in detail the steps involved in reforming and production of H_2, CO_2, and other light products.

In most cases the feedstocks to be converted contain a large amount of water, which in addition to serving as a solvent, can participate in the catalytic process.[7,8] Thus, to obtain accurate information regarding the catalytic chemistry of reforming oxygenated compounds, the influence of water must be considered. To this end the experiments reported herein were performed in liquid phase using water as the solvent. Furthermore, the presence of liquid water at high temperature may lead to dissolution of supports such as Al_2O_3. Therefore, in addition to performing the experiments in water we have studied changes in the oxide support for the Pt particles.

2. EXPERIMENTAL SECTION

2.1. Catalyst Synthesis. All the catalysis samples were prepared in a viscous flow atomic layer deposition (ALD) reactor.[14] The supports/substrates were placed in a resistively heated flow tube (1.4 in. ID). The flow reactor included independent reactant dispensers equipped with computer-controlled solenoid valves to inject precursors into the nitrogen carrier gas. High-area spherical alumina nanoparticles (BASF diameter ∼50 nm, surface area ∼40 m^2/g) were used for catalyst support. The alumina powder was loaded in a specially designed powder holder tray. The bottom tray of this fixture is constructed of 304 stainless steel with dimensions of 143 mm × 29 mm × 3.2 mm deep. The top of the powder fixture consists of a 200 × 600 mesh stainless steel wire cloth cover with 50% open area supported by a perforated stainless steel plate. The fine mesh cover prevents convective gas currents from disturbing the flat powder layer at the bottom of the powder tray, while allowing efficient diffusion of reactant and product gases in and out of the powder bed. By spreading the alumina powder into a thin layer, the diffusion of the ALD reactant gases between the alumina particles is relatively rapid. Ultrahigh purity (99.999%) nitrogen carrier gas was used at a flow rate of 360 sccm and a pressure of 1.3 Torr. Prior to coating, the alumina powder was cleaned in situ using a 10 min exposure to 400 sccm of 10% ozone in oxygen at the deposition temperature (150−300 °C) and a total pressure of 2.3 Torr.

2.2. Catalyst Testing System. Catalyst performance testing of the conversion of 1-propanol in liquid water was conducted in a high pressure tubular reactor (Figure 1). The reactants are introduced to the reactor by means of two syringe pumps (Teledyne-Isco, 100DM) that together can provide continuous, uninterrupted flow to the reactor. The outlet of the reactor passes through a back pressure regulator that controls reactor pressure, allowing the reactants to remain liquid at the reaction temperature (220−260 °C). After exiting the back-pressure regulator the effluent enters a vessel where the gas products are swept with a flow of dry N_2 and sent for gas chromatographic (GC) analysis. Liquid products remaining in the vessel are periodically sampled for analysis. The reactor system allows for treatment of the sample with hydrogen or nitrogen prior to the reforming experiments and without exposure to air.

The gas effluent was analyzed with an online GC system (Agilent 6890) equipped with both thermal conductivity and flame ionization detectors, and configured to detect both light inorganic gases (H_2, CO, CO_2, and N_2) and light hydrocarbons. Each of the liquid products was analyzed by gas chromatography−mass spectrometry (Agilent 6890). After product identification, the amount of propanol, propanal, and 2-methyl-2-pentenal was quantified by GC flame ionization detection (Agilent 5890) using 1-butanol as an internal standard. The propionic acid was quantified by a high performance liquid chromatography system (Agilent 1100)

dx.doi.org/10.1021/cs300405s | ACS Catal. 2012, 2, 2316−2326

equipped with a Bio-Rad HPX-87H (300 × 7.8 mm) column and a UV−vis detector (set to detect at 210 nm).

The solutions used for the catalytic experiments were prepared in advance using 1-propanol (Sigma-Aldrich, 99.9%) or propanal (Sigma-Aldrich, >97%) as received from the supplier and deionized water (18 MΩ-cm). After preparation, the solution was cooled to about 4 °C. The solution was then sparged with dry N_2 for >20 min to remove any traces of dissolved oxygen. This feed solution was then transferred into the syringe pumps without exposure to air; samples of the sparged solution were collected to perform conversion calculations.

The catalysts were mixed with SiC powder (100−140 mesh), and the mixture was placed between two pieces of glass wool inside a stainless steel reactor (ID = 0.152 in.), held in place by a piece of stainless steel tube on either side of the catalyst bed to minimize the reactor dead volume and prevent the catalyst bed from moving. Thermocouples were located inside the reactor on either side of the catalyst bed. Prior to reaction, each catalyst was treated in flowing H_2 (4% in helium) at 250 °C for 30 min and cooled to room temperature. The reactor was then filled with pure water and pressurized to 69 bar (1000 psi). Once pressurized and while under water flow (0.2 mL/min) the temperature in each of the zones of the furnace was adjusted so that the desired reaction temperature was reached as indicated by both thermocouples inside the reactor (above and below the catalyst bed). Following temperature stabilization the flow of the reactant mixture was initiated (typically 0.2 mL/min). Online GC samples were taken roughly every 17 min, and liquid samples were collected roughly every 50 min. Each time a liquid sample was collected, the gas−liquid separator was emptied and its contents weighed (to ensure mass balance closure).

Although all mass balances were high (95+%), the low conversions used in these experiments and the fact that propanol is highly volatile required its detection in both the liquid and the gas streams from the reactor outlet. Thus, direct calculation of the reaction rate proved unreliable, and all rates reported in this paper are based on the quantification of the gas and liquid products.

2.3. X-ray Absorption Spectroscopy (XAS). Pt L_3 X-ray absorption spectra were collected at beamlines 9-BM and 10-ID of the Advanced Photon Source at Argonne National Laboratory. The energy of the X-ray beam was selected by means of a Si (111) double crystal monochromator; the harmonics were removed from the beam by detuning to 60% at beamline 9-BM and using a Rh-coated mirror at beamline 10-ID. The X-ray absorption spectra were collected in transmission mode using three gas-filled ion chambers to measure the intensity of the X-rays before and after the sample, and after the reference. Platinum foil was scanned simultaneously with the sample to allow calibration of the energy scale. Since the foil spectrum was also used as a reference for the extended X-ray absorption fine structure (EXAFS) data fitting, care was taken to obtain good quality spectra of the Pt foil.

For characterization under reaction conditions, the sample was placed inside a vitreous carbon tube (Sigradur G Hochtemperatur-Werkstoffe; 10 mm OD × 4 mm ID × 200 mm long), which allows the high energy X-rays to pass through and can withstand pressures in excess of 30 bar (435 psi). The tube was connected to a flow system that allows pumping of high pressure liquids, analysis of the gas phase products, and collection of liquid samples.[15] The in situ experiment was performed by using the same steps as the catalyst testing. However, before starting reactant flow, catalyst samples were scanned at high temperature in flowing liquid water for roughly 2 h to assess the effect of water on the Pt particle size.

The fresh and spent catalyst samples from the performance testing and a sample with known adsorbates were characterized by pressing a small self-supporting wafer into a holder capable of fitting six samples.[16] The holder was placed inside a quartz tube attached to fittings that allow controlled atmosphere gas flow and scanning of each sample without exposure to air. Once inside the cell, the samples were heated in flowing H_2 (3.5 mol % in He) to 250 °C and then kept at that temperature for 30 min. The flow was then changed to pure He, and the sample was cooled to room temperature.

To interpret the X-ray absorption near edge structure (XANES) spectra of the catalyst characterized under reaction conditions, the catalyst sample was characterized with various adsorbed species. The spectra of each catalyst with adsorbed water were taken from the initial stages of the in situ experiment. The spectra of the sample with no adsorbates were taken by reducing the catalyst at 250 °C in H_2 followed by purging the cell with pure He for 10 min while the sample was still at high temperature. Spectra were then recorded with either adsorbed H_2 or CO (flowing 3.5% H_2 in He (Airgas) or 1% CO in He (Airgas)), where a 5-min gas introduction was followed by purging the sample cell with He before collecting the spectra.

2.4. Transmission Electron Microscopy (TEM). A suspension of catalyst powder (1−2 mg) in pure ethanol (1−3 mL) was dispersed by using an ultrasonic bath for about 5 min. Two to three drops of the resulting suspension were spread over a lacey carbon-coated copper mesh TEM grid (200 mesh). High resolution TEM images of the samples were taken on an FEI Titan apparatus operating at 300 kV and equipped with a Gatan Imaging Filter (GIF). The images were captured digitally on a CCD camera (1024 × 1024 pixel) and recorded with Gatan DigitalMicrograph software.

2.5. Extended X-ray Absorption Fine Structure (EXAFS) Spectroscopy. Averaging and initial data processing (rebinning) were performed with the software package Athena.[17] Data reduction to obtain the EXAFS spectra and fitting of the data were performed with the software package WinXAS.[18] The data were fitted by using the experimentally obtained references. The fitting was performed in *R*-space (where *R* is the interatomic distance) using at least two *k*-weightings of the data (k^2 and k^3) and determining that the data fit well in both cases. The fit was considered to be appropriate only if the fit parameters were physically reasonable: (1) the value of ΔE_0 was considered appropriate only if -10 eV $< \Delta E_0 < 10$ eV, and (2) the value of $\Delta\sigma^2$ was considered appropriate only if the magnitude was $0 < \Delta\sigma^2 < 1.5 \times 10^{-2}$ Å^{-2}.

2.6. X-ray Absorption Near Edge Structure (XANES) Spectroscopy. Data processing in the XANES region was performed with the Athena software package,[19] where the spectra were calibrated, averaged, and normalized, and the resulting spectra were exported to an Excel spreadsheet. Difference XANES (ΔXANES) spectra were obtained by subtracting each of the spectra from the spectrum of the supported Pt sample with no adsorbates (reduced and then treated in He at high temperature). The ΔXANES of the sample under reaction conditions was fitted by using a linear combination ΔXANES of the samples with known adsorbates

dx.doi.org/10.1021/cs300405s | ACS Catal. 2012, 2, 2316−2326

(H_2, CO, and H_2O); a least-squares method was used to minimize the error.

2.7. Particle Size Determination. Particle size distributions were determined from TEM micrographs directly (without any processing). Several micrographs (at least six) were used to determine the distribution of each sample. The image processing software GIMP was used to determine the size of each particle and calibrate the scale. The particle size distributions were calculated based on at least 450 measured particles for each sample.

3. RESULTS

3.1. Samples. Because of the possibility of leaching alumina during high-temperature liquid processing of water containing feedstocks, platinum was supported over alumina particles which were coated via ALD with insoluble metal oxides (TiO_2 and CeO_2) prior to the addition of the Pt. Table 1 summarizes each of the samples used for 1-propanol conversion along with the characteristics of any added oxide layer.

Table 1. Samples Used for the Conversion of 1-Propanol

sample name	metal	coating	support
Pt−Al	Pt (1 ALD cycle)	none	spherical Al_2O_3 (NanoDur)
Pt−Ce	Pt (1 ALD cycle)	CeO_2 (20 ALD cycles)	spherical Al_2O_3 (NanoDur)
Pt−Ti	Pt (1 ALD cycle)	TiO_2 (20 ALD cycles)	spherical Al_2O_3 (NanoDur)
Al_2O_3	none	none	spherical Al_2O_3 (NanoDur)

3.2. Catalyst Testing. *3.2.1. Activity for 1-Propanol Conversion.* Supported Pt samples were tested for the conversion of 1-propanol in liquid water at four temperatures (230, 240, 250, and 260 °C). Conversion at all temperatures tested were less than 10% with mass balances between 95% and 98%. The data indicate that all three catalysts tested (Pt−Al, Pt−Ti, and Pt−Ce; Table 1) were active for the conversion of 1-propanol. Table 2 shows the rate of each of the samples at 250 °C. The data indicate that Pt−Ti was the most active catalyst, followed by the Pt−Al sample, which has roughly half the rate of the Pt−Ti sample. The Pt−Ce sample has slightly lower activity than the Pt−Al sample. These results provide a strong indication that the TiO_2 coating on the alumina enhances the rate of the Pt clusters while the presence of CeO_2 has the opposite effect. No conversion of 1-propanol was observed when the Al_2O_3 support was used, implying that the supported Pt in the catalyst is the active phase.

3.2.2. Gas Phase Products of 1-Propanol Conversion. Table 2 also shows the selectivities for all the observed products, that is, (moles of product formed)/(moles of reactant consumed), of the reaction at 250 °C for each of the catalysts. Ethane and CO_2 are among the most abundant products. The presence of both products shows that the C_3 chain is cleaved adjacent to the C−O bond. Furthermore, regardless of the temperature, the C_2H_6/CO_2 ratio remains close to 1 (Figure 2), suggesting that the stoichiometry of these two compounds is fixed and also that the ethane does not further react. This inference is supported by the lack of detectable quantities of methane, a product from ethane cleavage or other compounds containing a C_2 backbone. Since the C_2H_6/CO_2 ratio is unaffected by the change in conversion (and temperature), we infer that both products are formed simultaneously.

Within the gas products, large amounts of H_2 were observed, as expected from the stoichiometry of the conversion of 1-propanol to CO_2 and ethane. However, the rate of H_2 production was, in all cases, more than twice that of ethane (or CO_2). Since conversion of 1 mol of propanol to 1 mol of ethane and 1 mol of CO_2 would produce 2 mols of H_2, these results suggest that at least part of the H_2 is formed prior to the reaction responsible for ethane formation.

Regardless of the catalyst, propane is also observed in the products, with selectivity roughly half that of ethane. The presence of propane shows that propanol was also directly deoxygenated, consuming one hydrogen molecule and producing a water molecule. Although it is possible that propane was formed from the dehydration of propanol to form propylene followed by hydrogenation (using the H_2 formed from propanol), the absence of any propylene product makes this possibility less likely. More likely is that the propane was formed by direct hydrodeoxygenation. Finally, the least likely possibility is that propane originates from the OH shifting to another propanol molecule, forming propane and a diol or other species containing two oxygenated carbon atoms. Diols are not observed in either the gas or the liquid phase products.

3.2.3. Liquid Phase Products of 1-Propanol Conversion. Propionaldehyde (or propanal) was one of the two products identified in the analysis of the liquid effluent. The presence of this product shows that the direct dehydrogenation of propanol is occurring, consistent with observation of hydrogen in the reactor effluent and with the inference that H_2 was formed in steps prior to ethane formation. The second product was

Table 2. Activity and Selectivity of Various Catalysts for Aqueous Phase Reforming of 1-Propanol and Propionaldehyde

			selectivity[e] at 250 °C (mol %)						
catalyst	reactant	rate (mol/s/g-cat) × 10^5	propanol	propanal	propane	propionic acid	2-methyl-2-pentenal	H_2	ethane
Pt−Al[a]	1-PrOH	4.9[c]		12	13	46		159	29
Pt−Ti[a]	1-PrOH	10.9[c]		10	12	48		164	30
Pt−Ce[a]	1-PrOH	4.1[c]		15	10	55		149	19
Al_2O_3[a]	1-PrOH	0[c]							
Pt−Al[b]	PrO	49[c,d]	52		0.4	30	<1	1.4	16
Al_2O_3[b]	PrO	5.5[c]	<1			0	99		0.2

[a]Conditions of experiment: 5 wt % 1-propanol in water, flowing at 0.2 mL/min with about 0.1 g of catalyst. [b]2% propanal in water flowing at 0.2 mL/min over 0.1 g of catalyst (when applicable). [c]Rates for the conversion of propanol were measured at 250 °C; for the conversion of propanal they were measured at 230 °C; all rates were calculated as the consumption of the reactant. [d]This value was measured at high conversion (65%); thus, it only represents a lower limit for the activity, and is only used for comparison. [e]The selectivity was calculated as the ratio of the rate of production of the product and the rate of consumption of the reactant.

dx.doi.org/10.1021/cs300405s | ACS Catal. 2012, 2, 2316−2326

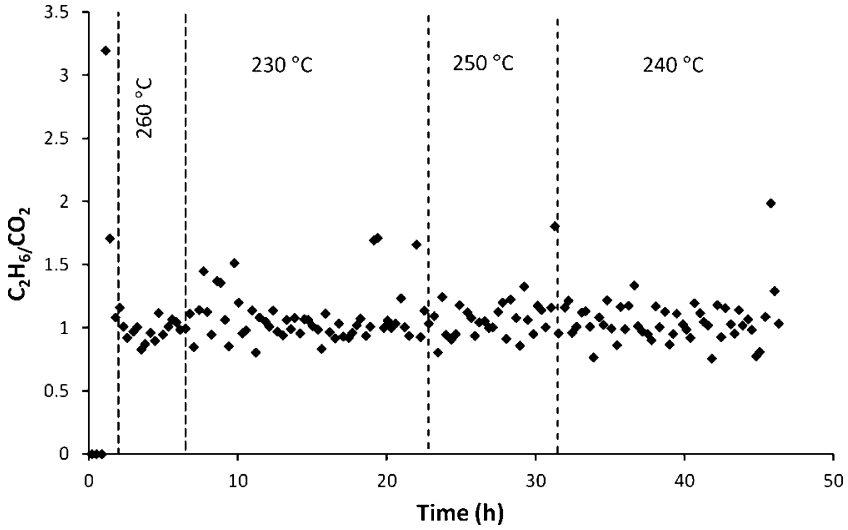

Figure 2. Selectivity ratio of CO_2 to ethane during the course of an entire experiment. During the experiment the temperature in the reactor was changed between 260 and 230 °C. The points during the first two hours correspond to the time it takes for the system to stabilize and the products to be collected.

propionic acid, which can be inferred to result from the oxidation of propionaldehyde. Propionic acid can readily decompose to form CO_2 and ethane through decarboxylation. The presence of this compound is consistent with an observation by Wawrzetz et al.[20] during the conversion of 1-propanol at 200 °C. However, neither the present experiment nor that of Wawrzetz et al.[20] can identify the source of the second oxygen in the acid. Finally, careful inspection showed no other alcohols or molecules with two oxidized carbons in the product stream, strongly suggesting that a bimolecular shift of the alcohol group was not a significant reaction under these conditions.

3.2.4. Reaction of Propanal. The conversion of propanal was studied to gain further insight regarding the reaction network of propanol reforming and to determine the source of oxygen in the formation of propionic acid. The Pt−Al catalyst was used to study this reaction. To obtain a broad range of conversions, the catalyst was tested at four reaction temperatures (240, 230, 200, and 190 °C).

The data show that at 240 °C the propanal is nearly completely converted to products (96% conversion), and even at the lowest temperature (190 °C) the conversion (10%) is beyond that observed at 260 °C for the conversion of 1-propanol (<5%). Since propanal is a primary product in the conversion of 1-propanol, this result demonstrates that the conversion of propanal is much faster than the dehydrogenation of propanol, and that the latter is rate determining in H_2 production. The gas phase products were H_2, CO_2, and C_2H_6, the same as for the conversion of 1-propanol. The selectivity ratio of H_2 to C_2H_6 is much lower than 1 (the highest value was 0.16 at 200 °C). This ratio contrasts with that observed during the propanol conversion (at any temperature) where the ratio was always >2, suggesting that little H_2 is produced after the first dehydrogenation.

Large amounts of propionic acid are formed during the conversion of propanal. The highest selectivity to propionic acid (55%) was seen at 200 °C, where the conversion was roughly 15%. Although the comparison of conversion at different temperatures is unreliable for determining the reaction pathway, the results show that propionic acid reacts further even at these low temperatures (<200 °C). This observation is consistent with the inference that propionic acid is only an intermediate product of the reforming process for 1-propanol, suggesting that decarboxylation of propionic acid is at least one major source of CO_2 and C_2H_6.

1-Propanol was also observed during propanal reforming. Since no H_2 was present in the initial reaction mixture, and H_2 was formed only in small quantities in the reaction, it is unlikely that this product would be formed by the direct hydrogenation of the aldehyde. At the highest temperature the selectivity to propanol was significantly higher than that of propionic acid, and at the lowest temperature (190 °C) (i.e., lowest conversion) the selectivities nearly matched, suggesting that the formation of one molecule of propionic acid is accompanied by the formation of one molecule of propanol. This finding implies that the aldehyde both oxidizes and reduces during the reaction—a Cannizzaro-like reaction.[21,22] This class of reactions has been reported to occur in basic solution (at moderate temperatures) and in supercritical water in the absence of added base.[23] An alternative to the Cannizzaro reaction is the Tishchenko route[22,24,25] that employs a surface bound metal alkoxide that could occur on the surface of the alumina. Therefore, it was necessary to determine whether the solid catalyst was responsible for these reactions or if this was a homogeneous reaction.

Experiments were carried out in the absence of catalyst and with only the alumina support. In both experiments no gas phase products were observed at any of the tested conditions. Liquid analysis revealed that some of the propanal is converted at these conditions, with the highest conversion being about 14% at 260 °C (20 °C higher than the rest of the propanal experiments). When alumina or no catalyst was used, the only observed product was 2-methyl-2-pentenal, an aldol condensation product. This result demonstrates that the formation of propanol and propionic acid from propanal was due to the Pt on the catalyst and did not occur in solution or on the support surface. Furthermore, the lack of 2-methyl-2-pentenal in the product when supported Pt was used as a catalyst is a strong indication that either this reaction is inhibited by the catalyst (unlikely) or that the rate is simply too low in comparison with

dx.doi.org/10.1021/cs300405s | *ACS Catal.* 2012, 2, 2316−2326

that of Cannizzaro-like reactions, which led to nearly 100% conversion at 240 °C.

3.3. Characterization. *3.3.1. EXAFS Characterization of Samples before and after Catalysis.* The best fit for the EXAFS data characterizing the Pt−Al sample (Table 3) before catalysis shows a single Pt−Pt contribution at 2.70 Å, indicating that after reduction the platinum is metallic. The fit also shows a coordination number of 8.2, suggesting that, on average, the particles were small, roughly 4 nm. Similarly, satisfactory fits were obtained of the spectra characterizing Pt−Ce and Pt−Ti samples with a single Pt−Pt contribution at approximately 2.70 Å and coordination numbers of 6.0 and 4.9, respectively.[26] The average cluster size is estimated roughly as 2 and 1 nm, respectively.

Table 3. EXAFS Fit Parameters for Supported Pt Samples before and after Use as Catalysts

sample	treatment	contribution[a]	N^b	R (Å)^b	$\Delta\sigma^2$ (Å^{-2})^b	E_0 (eV)^b
Pt−Al	none	Pt−Pt	8.2	2.70	0.0052	−2.38
	reforming at 250 °C for 7 h	Pt−Pt	11.8	2.76	0.0024	−0.46
	reforming at 250 °C for 29 h	Pt−Pt	11.4	2.74	0.002	−2.67
Pt−Ti	none	Pt−Pt	6	2.71	0.002	−1.7
	reforming at 250 °C for 9 h	Pt−Pt	10.9	2.77	0.0017	−0.1
Pt−Ce	none	Pt−Pt	4.9	2.67	0.002	−4.6
	reforming at 250 °C for 13.5 h	Pt−Pt	11.4	2.74	0.001	−2.4

[a]Only Pt−Pt contributions were necessary to fit the spectra of each sample. [b]The estimated accuracies for each parameter are as follows: N, ± 10%; R, ± 0.02 Å; $\Delta\sigma^2$, ± 20%; ΔE_0, ± 20%.

Results from fitting EXAFS spectra characterizing the three samples after they were used for the conversion of 1-propanol (Table 3) show a single Pt−Pt contribution at approximately 2.75 Å, consistent with the interatomic distance of bulk platinum. The Pt coordination numbers were 11.8, 10.9, and 11.4 for Pt−Al, Pt−Ti, and Pt−Ce, respectively. As a result of the inherent error in EXAFS, any calculation of particle size using such coordination numbers is unreliable. Nonetheless, it is clear from the results that, on average, the Pt particles suffered severe sintering under reaction conditions. However, it is unclear if this sintering was caused by the presence of hydrogen, a product of the reaction, in the stream or simply the presence of an extremely high concentration of water at high temperature.

3.3.2. TEM Characterization of Used and Fresh Catalysts. Although EXAFS provides a rough estimate of the average size of the Pt particles, TEM is needed to determine the distribution of particle sizes. The Pt particle size distribution of the Pt−Al sample shows an average particle size of 3.4 nm with a relatively broad distribution (Figure 3A) (σ = 2.6 nm). Furthermore, about 4% of the particles observed were significantly larger than the rest (>10 Å).

The TEM micrographs of the Pt−Ce sample before reaction revealed an average particle size of 1.6 nm with a distribution (Figure 3B) that is significantly narrower (σ = 0.43 nm) than that of Pt−Al. Also, no large particles (>10 Å) were observed in the >500 particles counted, suggesting that if such particles are present they are extremely rare. This result is consistent with the EXAFS results showing that the fresh Pt−Ce sample contained, on average, smaller particles (as reflected by a lower Pt−Pt coordination number) than Pt−Al.

Similar to the sample with CeO_2 coating, TEM characterization of the Pt−Ti showed an average particle size of 2.1 nm, with a fairly narrow distribution (Figure 3C) (σ = 0.50 nm). This result shows that a coating of TiO_2 on the surface, as with the CeO_2 coating, allows a better dispersion of the Pt. Furthermore, of the >450 particles counted for this sample, none exceeded 10 nm in size.

The particle size distribution of the Pt−Al sample after 1-propanol reforming (Figure 3A) has an average particle size approximately 1 nm greater than before reaction. Although still low, the number of large particles (>10 Å) grew significantly from about 4% to about 8%, with the largest observed particle being 28 nm in diameter. This significant change is the major contributor to the dramatic increase in the Pt−Pt coordination number observed in the EXAFS data. Furthermore, we believe that this result implies that the growth of the Pt particles is not due to a uniform increase in the size of the particles but to agglomeration of individual small particles.

The particle size distribution of the Pt−Ce and Pt−Ti samples (Figure 3D) after 1-propanol reforming shows that the average Pt particle size is roughly 2.9 nm. In addition, the histograms show a significantly broader distribution compared to that of the fresh sample. The Pt−Ti sample shows no evidence of any particles >10 nm, while for the Pt−Ce sample, some >10 nm particles were observed (0.8%), with the largest being about 22 nm in diameter.

3.3.3. In Situ EXAFS Characterization. To understand the sintering behavior, XAS spectra were collected while the Pt−Ce sample was kept in water at 230 °C. Fitting of the EXAFS region of the spectra shows that the Pt−Pt coordination number increases from 7.7 to 8.8 over a period of about 2 h (Figure 4), corresponding to an increase in particle size from 3.5 to 5.2 nm. This result shows that in the presence of high-temperature liquid water, even in the absence of hydrogen, Pt clusters rapidly sinter and form significantly larger clusters. A corollary of this result is that the presence of liquid water leads to the rapid loss of active (surface) Pt. It should be pointed out that this two hour sintering occurs before the first catalyst activity test is taken. Therefore the activity data shown in Table 2 is after sintering has occurred. Hence, one of the challenges in the synthesis of catalysts for liquid processing of feedstocks derived from biological sources (which contain water) is to prevent sintering in the harsh processing conditions.

3.3.4. In Situ XANES Characterization. The XANES region of the XAS spectra that were collected for the Pt−Ce sample with known adsorbates (Figure 5A) shows that the nature of the adsorbed species can greatly influence the electronic structure of the Pt particles. Specifically, the XANES results show that the presence of adsorbed CO leads to a growth of the white-line intensity, a shift in the edge position, and a broadening of the white line relative to the Pt sample without CO. The ΔXANES spectra of the sample after each adsorbate is added (and using the Pt catalyst under He at room temperature as a standard) are characterized by significantly different shapes and sizes, depending on which adsorbate is on the Pt surface (Figure 5B). Consequently, each ΔXANES spectrum can serve as a reference to determine which species are present on the sample under reaction conditions.

dx.doi.org/10.1021/cs300405s | ACS Catal. 2012, 2, 2316−2326

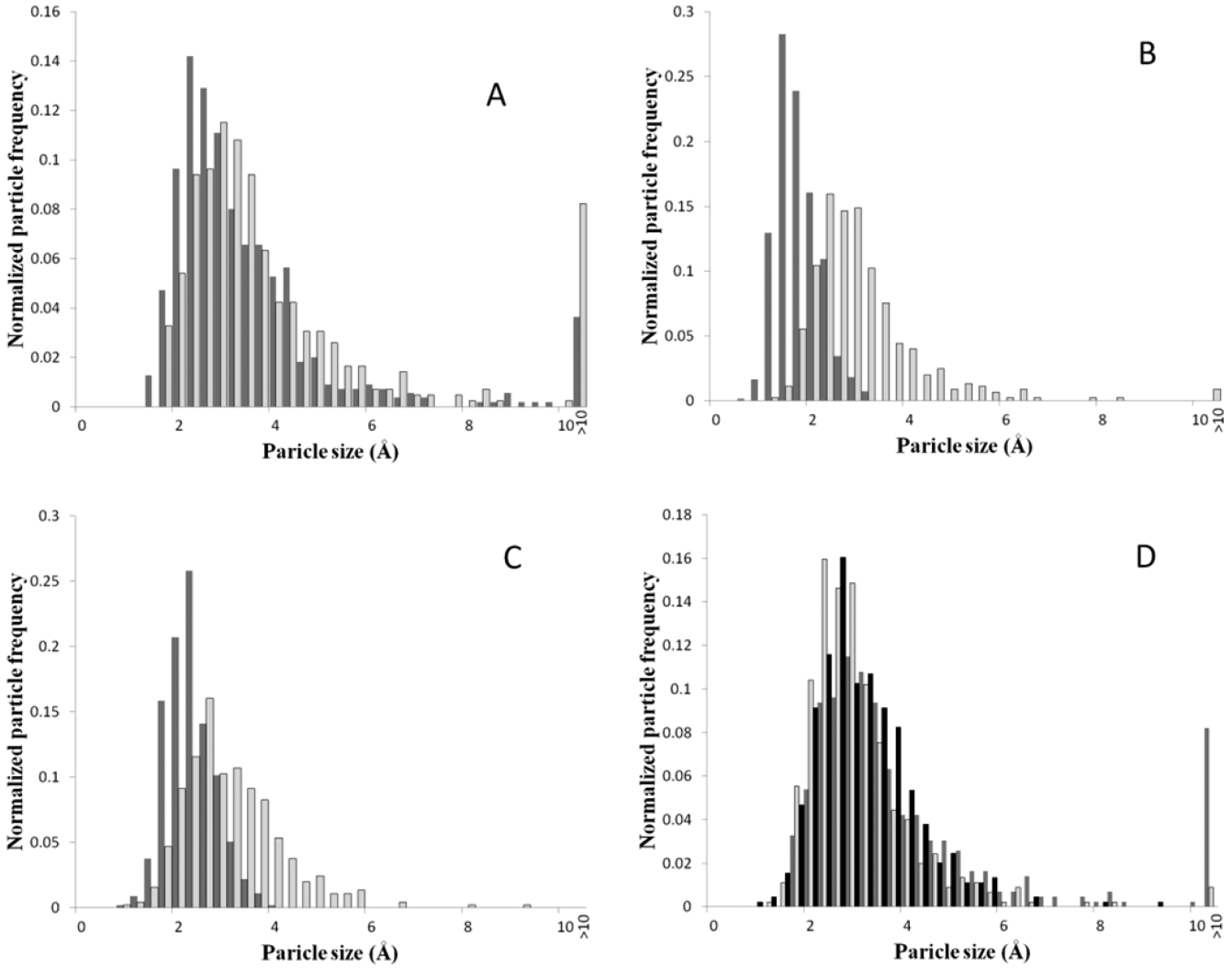

Figure 3. Particle size distributions of supported Pt catalysts before (light bars) and after (darker bars) 1-propanol reforming: (A) Pt−Al sample, (B) Pt−Ce sample, and (C) Pt−Ti sample. (D) Supported Pt samples after 1-propanol reforming: Pt−Ce (light gray), Pt−Al (dark gray), and Pt−Ti (black).

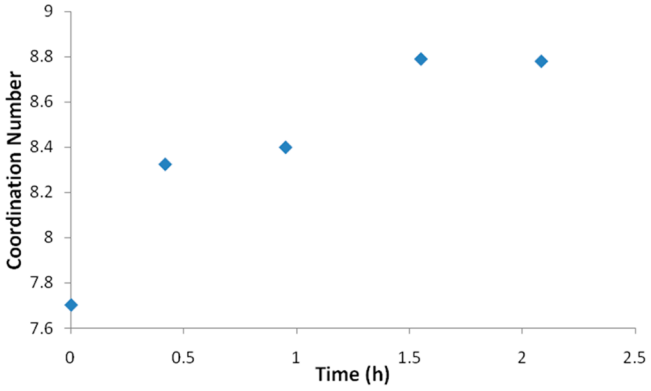

Figure 4. Pt−Pt coordination number of Pt−Ce sample while in liquid water at 230 °C.

A linear combination of the spectra characterizing the samples with known adsorbates was used to model that of the sample under reaction conditions. The ΔXANES fit provides information about the most abundant surface species under reaction conditions (Figure 6) and shows that the latter can be explained by 96% of the spectra of H_2O, 43% of the spectra of the sample exposed to CO, and 19% of the spectra of H_2. Since reference spectra correspond to samples with unknown surface coverage of adsorbates, these values correspond to fractions of the surface coverage attained for each reference, and not percentages of the absolute surface coverage. Thus, the results show that the amount of adsorbed water is nearly the same as when the sample is under pure water at 230 °C, which is as expected since the reactant mixture is roughly 95 wt % water. Also, the coverage of H_2 in the sample under reaction conditions is 19% that of a sample exposed to 3.5% H_2 in helium at room temperature, and not 19% of the total metal surface. Finally, the results also show a low yet appreciable amount of CO on the surface of the Pt clusters, suggesting that CO is being produced by the reaction. The finding that CO was not observed in the chromatographic analysis of the gas products further suggests that either it is being converted to CO_2 or, if present in the products, it would be at very low concentration.

4. DISCUSSION

4.1. Oxidation of Carbon Backbone. Reforming of 1-propanol generates propionic acid as an intermediate in the

dx.doi.org/10.1021/cs300405s | ACS Catal. 2012, 2, 2316−2326

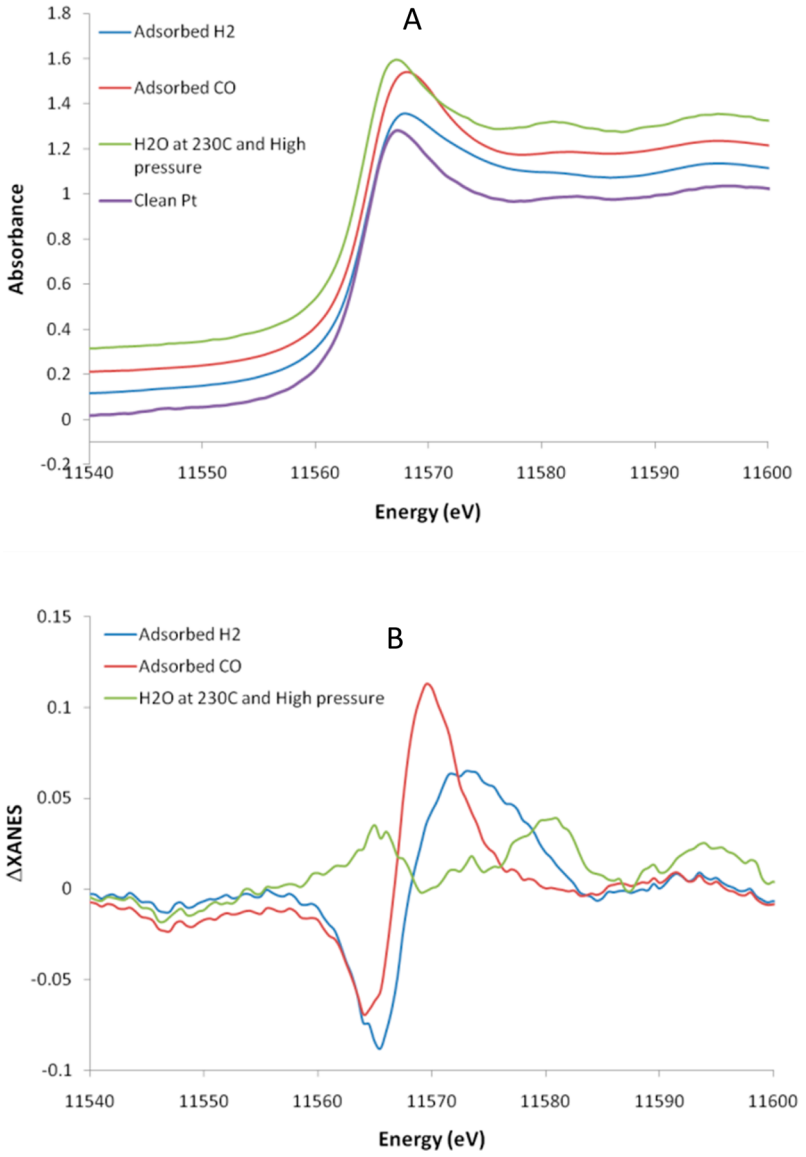

Figure 5. Pt−Ce sample after exposure to the adsorbates CO, H_2, and water: (A) XANES spectra of sample before and after exposure and (B) difference XANES (ΔXANES) spectra of the sample with each of the adsorbates minus that of the sample with no adsorbates.

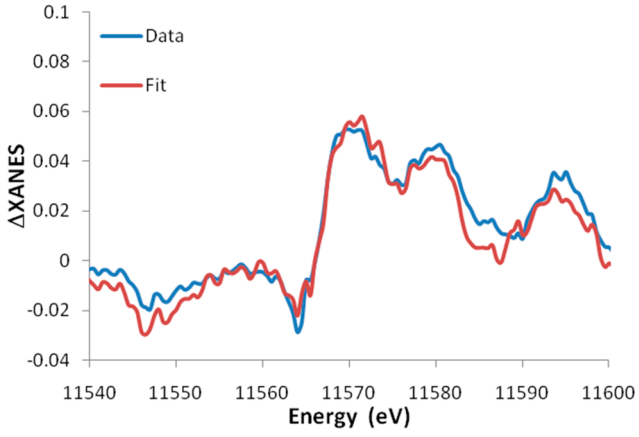

Figure 6. ΔXANES spectra of the Pt−Ce sample during the conversion of 1-propanol at 230 °C and 30 bar and spectra resulting from the linear combination of spectra of Pt−Ce sample with known adsorbates.

formation of CO_2 and ethane. Although the presence of propane might suggest that part of the propanol was reduced by the aldehyde leading to the formation of propane and propionic acid, the amount of propane formed was, in all cases, significantly lower than the amount of acid observed (despite the fact that the acid can be further converted to CO_2, and the propane does not react further). Furthermore, when propanal alone was used as a reactant, the amount of propane produced was practically zero while the amount of acid produced was large (roughly 30% selectivity at 230 °C), suggesting that propanol (or propanal) is not the source for the second oxygen in the acid. This observation is further supported by the lack of evidence of other products, such as 2-propanol, that are characteristic of such an OH shift.

The conversion of propanal leads to a large amount of propanol being produced, with the propanol-to-propionic acid ratio being about 1.0 at 190 °C (25% conversion) and about 1.7 at 240 °C (95% conversion). It is clear from the presence of these two products (1-propanol and propionic acid), coupled with the presence of water and lack of O_2 in the system, that

dx.doi.org/10.1021/cs300405s | ACS Catal. 2012, 2, 2316−2326

one molecule of propanal is oxidized to form the acid with the water acting as the source of the second oxygen, while another propanal molecule is reduced to the alcohol. These products are characteristic of Cannizzaro reactions.

Although Cannizzaro reactions typically occur at mild conditions (~80 °C) in a basic environment,[27] in recent years it has been reported that such transformations can occur in supercritical water without the addition of base to the solution.[23] This reaction occurs, in part, resulting from the higher concentration of OH^- ions in solution because of the higher dissociation constant of water (at high temperatures).[28] However, when similar experiments were conducted at lower temperature (250 °C),[23] no evidence for a Cannizzaro reaction was observed.

Typically at conditions necessary to perform Cannizzaro reactions (basic medium and mild temperature), the presence of C−H bonds α to the carbonyl group (as is the case in propanal) leads to aldol condensation, which would dominate the selectivity. During the conversion of propanal, with the supported Pt catalyst, no evidence of aldol condensation products was observed. Furthermore, without Pt (no catalyst or only the support), small amounts of 2-methyl-2-pentenal (an aldol condensation product) were observed (at 260 °C), showing that in solution condensation is the preferred reaction, and that the Al_2O_3 alone is not responsible for the Canizzarro-like reaction. The latter result is consistent with the observations of Nagai et al., who saw aldol condensation as the only reaction of ethanol occurring in water at 250 °C.[23] Thus, it is clear that aldol condensation is one of the routes for conversion of propanal. However, in the presence of platinum, this reaction is extremely slow relative to the Cannizzaro-like reaction, and thus no aldol condensation products were observed. Furthermore, unlike typical Cannizzaro reactions, the conversion of propanal to propanol and propionic acid appears to be catalyzed by the Pt, and not OH^- alone. Evidently, the presence of water is necessary for the reaction (since it is one of the reactants); however, the necessity for OH^- is still unclear. The combination of OH groups on the support and the metal sites may be sufficient to perform this conversion. Further experiments are needed to test this possibility.

The occurrence of Cannizzaro-like reactions during propanal conversion leads to the formation of propanol and propionic acid from propanal. Since this reaction is apparently very fast, as evident from the high conversions (65%) of propanal even at 230 °C (where only low 1-propanol conversions are observed), it is possible that little to no decarbonylation occurs, and that all the CO_2 and ethane are produced from the acid. This inference is supported by the low hydrogen-to-CO_2 ratio (0.06 at 230 °C) observed during propanal conversion. A corollary of this idea is that the production of hydrogen is accelerated by the presence of water in the system, since it opens a new pathway for the formation of propanol and the formation of more H_2.

A second possibility has also been recently suggested is the so-called Tishchenko reaction. This reaction that involves disproportionation of an aldehyde lacking a hydrogen atom in the α position in the presence of an alkoxide.[25] The reaction product is an ester. Typical catalysts are aluminum alkoxides or sodium alkoxides. In the current case two propanal molecules can couple to make propyl propionate. The propyl propionate would then be hydrolyzed to propionic acid and propanol. Future studies will investigate this further.

4.2. H_2 Production. Hydrogen is produced in the early stages of the conversion of 1-propanol; this conclusion is clear from the concentration of hydrogen observed relative to any other product in the reaction. In particular, the hydrogen concentration was more than twice the amount of ethane (or CO_2) observed at any given time with all catalysts, while the expected ratio from the full conversion of propanol to CO_2 and ethane is two. The H_2-to-CO_2 ratio decreased at higher reaction temperatures (higher conversions) as expected when forming either the propionic acid or the propanal as intermediates. The resulting hydrogen deficient carbon rich species in the liquid phase release the majority of the H_2 gas. The presence of propanal further bolsters this inference and is evidence that H_2 is formed in the first step of the reforming process, which explains the high amounts of H_2 observed.

Hydrogen can potentially be produced via two routes, dehydrogenation of 1-propanol and water-gas shift (following decarbonylation). However, the nearly equal amounts of propanol and propionic acid produced at the lowest temperature (i.e., lowest conversion) during propanal conversion suggest that, although the hydrogenation/dehydrogenation reaction at the current conditions favors the formation of propanol the majority of propanol is produced by the Cannizzaro-like reaction. Therefore, the lack of hydrogen during propanal conversion is likely due to H_2 not being produced rather than consumption of hydrogen through hydrogenation. This result implies that the low amounts of H_2 observed are due to the decarbonylation reaction occurring at low rates relative to the Cannizzaro-like reaction.

It follows from the previous suggestion that the primary reaction responsible for the formation of hydrogen during propanol conversion is the dehydrogenation of propanol, and that the decarbonylation of propanal is relatively slow. This suggestion is consistent with the large amount of propionic acid observed at practically all temperatures during propanal conversion; it is also consistent with the high propionic acid-to-propanal ratios observed during propanol conversion. However, despite the apparently dominant role of the Cannizzaro reaction in the formation of H_2, ethane, and CO_2, the route involving decarbonylation might contribute to H_2 formation.

Although the principal reaction of propanol is dehydrogenation to form propanal, there is also evidence of a significant quantity of propane (10−15%) being formed. This deoxygenation reaction leads to the formation of water and the consumption of hydrogen. Although at first glance this reaction appears detrimental because of H_2 consumption, the lower hydrogen production leads to products with a more stable carbon backbone, which could be useful under certain circumstances.

4.3. Water-Gas Shift (WGS) Reaction. Although the bulk of the hydrogen formation is due to the dehydrogenation of the alcohol group in propanol, and WGS is not the major contributor to H_2 production, characterization of the catalyst under reaction conditions does show the presence of CO adsorbed on the Pt surface. This observation has two possible explanations: (1) CO is slowly produced by decarbonylation and, therefore, WGS occurs slowly, or (2) CO could be produced through reverse WGS from CO_2 and H_2, and could only be present on the surface of the catalyst.

Regardless of the origin, CO binds strongly enough to the Pt surface to be observed in the XANES spectra, but is present in such low concentrations as not to be detected in the gas phase.

The implication of this strong binding is that CO molecules are acting as a poison for the catalyst by blocking active Pt sites. Thus, one of the aims of future catalyst design should be to prevent such poisoning behavior. To do so, the electronic properties of the Pt catalyst can be altered by adding a new metal and forming alloys. If properly done, this step could reduce the binding energy of CO and reduce the poisoning effect.

4.4. C−C Bond Cleavage. The presence of both CO_2 and ethane (a C_2 hydrocarbon) demonstrates that scission of C−C bonds occurs at the carbon that is bound to oxygen. The results also show that the ratio of CO_2 to ethane remains at about 1 under all conditions, suggesting that the stoichiometry of these two products is fixed. Thus, we infer that both CO_2 and ethane are formed in the same process, and that neither is further consumed. This inference is supported by the lack of evidence of any methane in the outlet stream, and the finding of no formation of heavier hydrocarbons. It thus follows that ethane is not further converted, and that under the reaction conditions studied (230−260 °C, liquid water) only bonds that involve an oxygenated hydrocarbon are labile enough to be cleaved.

4.5. Reaction Pathway. Combining all the information from the various experiments results in a relatively detailed picture of the reaction pathway for propanol reforming (Scheme 1). In this pathway, the major source of hydrogen is

Scheme 1. Pathway for the Conversion of 1-Propanol[a]

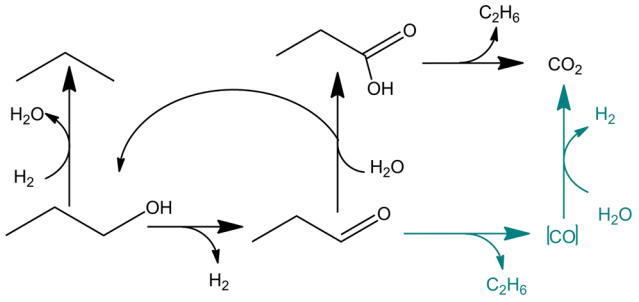

[a]The routes in lighter color are those expected to be minor contributions to the formation of CO_2.

the initial dehydrogenation of the propanol, rather than the result of decarbonylation followed by WGS, implying that the production of H_2 does not require a single C−C bond scission step. Furthermore, the results indicate that the relative stability of each of the C−C bonds plays a role in the reaction, and Scheme 1 shows both the paths of producing more hydrogen (less stable organics) and the consumption of H_2 (more stable organics). Both reactions occur simultaneously. Thus, designing a catalyst to accurately drive the selectivity to the desired product is a challenge.

The ability of the supported Pt to catalyze either the Cannizzaro or the Tischchenko reaction provides the necessary 1-propanol to produce twice the amount of hydrogen than would be produced by a single dehydrogenation step. This same reaction also forms acid in the absence of other oxygen sources. Additionally, the availability of this reaction leads to an acceleration of the H_2 production rate.

4.6. Sintering. Characterization of the Pt−Ce sample exposed to high temperature liquid water revealed that the particles sinter significantly in a short time (2 h led to an increase in size of about 40%). Therefore, in the design of industrial catalysts, the loss of exposed Pt becomes a concern since even at short times most of the Pt will be unavailable to catalyze the reaction. Furthermore, the in situ characterization shows that the sintering occurs in the presence of only water, implying that any catalyst used for conversion of biologically derived feedstocks that include or produce water will face such problems.

4.7. Effect of Catalyst Composition. Characterization through EXAFS and TEM of the samples before reaction made it clear that the coating of Al_2O_3 with both CeO_2 and TiO_2 leads to better dispersed Pt particles than those observed on Al_2O_3 with no coating. This effect is especially true for the presence of large Pt particles (>10 nm), which were observed on the uncoated sample but were absent in the samples coated with CeO_2 and TiO_2. However, once the samples were used in aqueous phase reforming, the Pt particles sintered and led to samples with very similar particle size distributions, in the 0−10 nm range. This finding implies that neither the CeO_2 or TiO_2 coatings provided sufficient stabilization of the Pt particles to prevent sintering. Some differences were observed, however, between the various samples. Although not distinguishable with XAS, TEM showed that the amount of >10 nm diameter particles changed depending on the coating of the sample in the order Pt−Al > Pt−Ce > Pt−Ti.

Taken together, the findings indicate that ALD coatings can potentially be used to produce highly stable metal particles by using a combination of layers of different materials to provide adequate anchoring of the particles and prevent their sintering. ADL does, however, affect the size of the starting Pt particle more than the final size after the reforming reactions. Adding layers that promote Pt anchoring (such as TiO_2) below the particles (achieved by adding it before Pt is added) and/or around the particles as an oxide that Pt does not readily anchor to may help stabilize the particles and minimize their migration.

Similar to the changes in particle size, the activity of the catalyst dramatically changed with the various coating materials. The activity was found to be Pt−Ti > Pt−Al > Pt−Ce. Thus, the dispersion of the Pt particles does not appear to be the sole factor that affects the activity for 1-propanol reforming and production of H_2. It is likely that the support changes the electronic properties of the particles.

5. CONCLUSIONS

Processing of biomass into transportation fuels will require large amounts of hydrogen. Most (if not all) of this hydrogen must be derived from biomass to maintain the "greenness" of the process. This work has shown that supported platinum can effectively dehydrogenate short chain alcohols (such as propanol) with relatively high selectivity. It is speculated that propanol is a good surrogate molecule for glycerol, which should be in plentiful supply from biomass processing.

The current paper has shown that the dehydrogenation of propanol goes through several competing reactions. The major source of hydrogen is the initial dehydrogenation of the propanol, leading to a mole of hydrogen for every mole of propanol consumed. This reaction results in a propanal intermediate that can be hydrolyzed to propionic acid. The propionic acid has been shown to rapidly decarboxylate to ethane and CO_2 with no net change in the hydrogen yield. A secondary, apparently minor, reaction of the propanal has been proposed to yield CO and ethane. Since no CO is observed, the CO likely reacts with the high concentration of water via WGS to yield more hydrogen and CO_2. A key for future catalysts is to

dx.doi.org/10.1021/cs300405s | ACS Catal. 2012, 2, 2316−2326

decrease the non-hydrogen producing decarboxylation reaction while improving the decarbonylation/WGS route.

Finally, a primary problem with all catalysts studied is the sintering of the metals under hydrothermal processing conditions. High pressure liquid water is a highly corrosive environment for supported metals. Future work will require supports (such as TiO_2) that can stabilize the active metal without negatively affecting the catalyst selectivity.

AUTHOR INFORMATION

Corresponding Author

*E-mail: marshall@anl.gov.

Funding

This material is based upon work supported as part of the Institute for Atom-efficient Chemical Transformations (IACT), an Energy Frontier Research Center funded by the U.S. Department of Energy, Office of Science, Office of Basic Energy Sciences. Argonne National Laboratory, a U.S. Department of Energy Office of Science laboratory, is operated under Contract No. DE-AC02-06CH11357.

Notes

The authors declare no competing financial interest.

ACKNOWLEDGMENTS

Use of the Advanced Photon Source, an Office of Science User Facility operated for the U.S. Department of Energy (DOE) Office of Science by Argonne National Laboratory, was supported by the U.S. DOE under Contract No. DE-AC02-06CH11357. MRCAT operations are supported by the Department of Energy and the MRCAT member institutions.

REFERENCES

(1) Huber, G. W.; Iborra, S.; Corma, A. *Chem. Rev.* **2006**, *106* (9), 4044−4098.

(2) Román-Leshkov, Y.; Barret, C. J.; Liu, Z. Y.; Dumesic, J. A. *Nature* **2007**, *447* (7147), 982−985.

(3) Chheda, J. N.; Huber, G. W.; Dumesic, J. A. *Angew. Chem., Int. Ed.* **2007**, *46* (38), 7164−7183.

(4) Dasari, M. A.; Kiatsimkul, P.-P.; Sutterlin, W. R.; Suppes, G. J. *Appl. Catal., A* **2005**, *281*, 225−231.

(5) Manzer, L. E. *Production of 5-methylbutyrolactone from levulinic acid*. U.S. Patent 6,617,464, September 9, 2003.

(6) Cortright, R. D. Dumesic, J.A. *Method for catalytically reducing carboxylic acid groups to hydroxyl groups in hydroxycarboxylic acids*. U.S. Patent 6,455,742, September 24, 2002.

(7) Akiya, N.; Savage, P. E. *Chem. Rev.* **2002**, *102*, 2725−2750.

(8) Cortright, R. D.; Davda, R. R.; Dumesic, J. A. *Nature* **2002**, *418*, 964−967.

(9) Vaidya, P. D.; Rodrigues, A. E. *Chem. Eng. Technol.* **2009**, *32* (10), 1463−1469.

(10) Iriondo, A.; Barrio, V. L.; Cambra, J. F.; Arias, P. L.; Güemez, M. B.; Navarro, R. M.; Sánchez-Sánchez, M. C.; Fierro, J. L. G. *Top. Catal.* **2008**, *49*, 46−58.

(11) Iriondo, A.; Cambra, J. F.; Barrio, V. L.; Güemez, M. B.; Arias, P. L.; Sánchez-Sánchez, M. C.; Navarro, R. M.; Fierro, J. L. G. *Appl. Catal., B* **2011**, *106*, 83−93.

(12) Ouyang, K.; Huang, Y.; Chen, H.; Li, T.; Cao, F.; Fang, D. *Front. Chem. Sci. Eng.* **2011**, *5*, 67−73.

(13) Torres, A.; Roy, D.; Subramanian, B.; Chaudhari, R. V. *Ind. Eng. Chem. Res.* **2010**, *49*, 10826−10835.

(14) Elam, J. W.; Groner, M. D.; George, S. M. *Rev. Sci. Instrum.* **2002**, *73* (8), 2981−2987.

(15) Fingland, B. R.; Ribeiro, F. H.; Miller, J. T. *Catal. Lett.* **2009**, *131* (1−2), 1−6.

(16) Castagnola, N. B.; Kropf, A. J.; Marshall, C. L. *Appl. Catal., A* **2005**, *290*, 110−122.

(17) Ravel, B.; Newville, M. *J. Synchrotron Radiat.* **2005**, *12*, 537−541.

(18) Ressler, T. *J. Synchrotron Radiat.* **1998**, *5*, 118−122.

(19) Ravel, B.; Newville, M. *J. Synchrotron Radiat.* **2005**, *12*, 537−541.

(20) Wawrzetz, A.; Peng, B.; Hrabar, A.; Jentys, A.; Lemonidou, A. A.; Lercher, J. A. *J. Catal.* **2010**, *269*, 411−420.

(21) Cannizzaro, S. *Liebigs Ann.* **1853**, *88*, 129−130.

(22) Sad, M. E.; Neurock, M.; Iglesia, E. *J. Am. Chem. Soc.* **2011**, *133* (50), 20384−20398.

(23) Nagai, Y.; Wakai, C.; Matubayasi, N.; Nakahara, M. *Chem. Lett.* **2003**, *32*, 310−311.

(24) Hattori, H. *Chem. Rev.* **1995**, *95* (3), 537.

(25) Tishchenko, V. *J. Russ. Phys. Chem. Soc.* **1906** *38*, pp 355, 482, 540, 547.

(26) Miller, J. T.; Kropf, A. J.; Zha, Y.; Regalbuto, J. R.; Delannoy, L.; Louis, C.; Bus, E.; van Bokhoven, J. A. *J. Catal.* **2006**, *240* (2), 222−234.

(27) March, J. *Advanced Organic Chemistry*; John Wiley & Sons: New York, 1992.

(28) Marshall, W. L.; Franck, E. U. *J. Phys. Chem. Ref. Data* **1981**, *10*, 295−304.